Injectable Disc-Derived ECM Hydrogel Functionalised with Chondroitin Sulfate for Intervertebral Disc Regeneration

Chiara Borrelli M.Sc. [1,2], and Conor T. Buckley, Ph.D.[1,2,3,4*]

[1] Trinity Centre for Biomedical Engineering, Trinity Biomedical Sciences Institute, Trinity College Dublin, The University of Dublin, Dublin, Ireland

[2] School of Engineering, Trinity College Dublin, The University of Dublin, Dublin, Ireland

[3] Advanced Materials and Bioengineering Research (AMBER) Centre, Royal College of Surgeons in Ireland & Trinity College Dublin, The University of Dublin, Dublin Ireland

[4] Department of Anatomy and Regenerative Medicine, Royal College of Surgeons in Ireland, 121/122 St. Stephen's Green Dublin 2, Ireland

*Corresponding author: Conor T. Buckley

E-mail address: conor.buckley@tcd.ie

Address: Trinity Centre for Biomedical Engineering

Trinity Biomedical Sciences Institute

Trinity College Dublin

Ireland

Telephone: +353-1-896-2061

Fax: +353-1-679-5554

Key words: hydrogel; repair; cell; biomaterial; spine; self-assembly

Running Header: Functionalised ECM for disc regeneration

Abstract

Low back pain resulting from intervertebral disc (IVD) degeneration is a significant socioeconomic burden. The main effect of the degeneration process involves the alteration of the nucleus pulposus (NP) via cell-mediated enzymatic breakdown of key extracellular matrix (ECM) components. Thus, the development of injectable and biomimetic biomaterials that can instruct the regenerative cell component to produce tissue-specific ECM is pivotal for IVD repair. Chondroitin sulfate (CS) and type II collagen are the primary components of NP tissue and together create the ideal environment for cells to deposit de-novo matrix. Given their high matrix synthesis capacity potential post-expansion, nasal chondrocytes (NC) have been proposed as a potential cell source to promote NP repair. The overall goal of this study was to assess the effects of CS incorporation into disc derived self-assembled ECM hydrogels on the matrix deposition of NCs. Results showed an increased sGAG production with higher amounts of CS in the gel composition and that its presence was found to be critical for the synthesis of collagen type II. Taken together, our results demonstrate how the inclusion of CS into the composition of the material aids the preservation of a rounded cell morphology for NCs in 3D culture and enhances their ability to synthesise NP-like matrix.

1. Introduction

The intervertebral disc (IVD) is a highly hydrated fibro-cartilaginous tissue critical for the normal functioning of the spine. There is still no accepted consensus with respect to the biochemical, mechanical and nutritional mechanisms that triggers degeneration of the IVD. However, it is clear that one of the effects of this process is the cell-mediated enzymatic breakdown of key extracellular matrix (ECM) components [1] and that it prevalently occurs in the nucleus pulposus (NP) of the disc [2-4]. The healthy NP consists of a network of highly hydrated sulfated glycosamminoglycans (sGAG) embedded in a loose type 2 collagen structure [5, 6]. Chondroitin sulfate (CS) is the most abundant sGAG and is responsible for the high levels of hydration of the tissue and resulting biomechanical properties to withstand compressive loads [7]. During disc degeneration (DD) the sGAG content of the NP decreases resulting in reduced water content, and concomitant functional capacity [2, 8].

Injectable biomaterials have been widely investigated in an attempt to restore or recreate the structural and biochemical composition of a damaged tissue, while at the same time having the advantage of being minimally invasive. Although a wide range of natural and synthetic polymers have been employed in tissue engineering, materials derived from the decellularisation of tissue specific ECM have received considerable attention in the last decade due to their high biocompatibility, excellent tissue integration, and intrinsic bio-inductive factors that can induce differentiation or promote a specific phenotype [9-18]. However, a major challenge of the decellularisation process is preserving the biochemical composition of the native tissue. During a standard decellularisation procedure native tissues are generally immersed into a series of water-based solutions. Due to their polar nature, GAGs are characterised by high water solubility and tend to disperse into the decellularisation solutions, compromising the integrity of the native tissue composition. Therefore, in order to retain the biomimetic composition of the material, it is necessary to reintroduce the fraction of GAGs lost

during the processing of the ECM, and more specifically CS. The presence of CS has been shown to have a positive effect in increasing matrix production, providing chondro-protection and anti-inflammatory properties [19-22]. Nevertheless, it is widely known that the presence of GAGs influences collagen fibril formation, with fibril networks forming less readily in a carbohydrate rich environment resulting in hydrogels with diminished integrity and poor mechanical properties [23-26]. Previous work has shown that carboxyl activated or functionalised CS can be combined with collagen to form self-crosslinkable hydrogel systems [27] overcoming the challenge of producing ECM-CS gels with poor mechanical properties and stability.

In the research of an appropriate cell source for the regeneration of the disc a number of important factors, such as potential immune rejection, technical and regulatory issues of utilising allogeneic donor cells, make the use of a patient's own cellular material an obvious choice [28]. Among the alternative cell sources discussed and analysed in literature, nasal septal cartilage may provide for an attractive tissue source. This tissue is easily accessible to harvest under local anaesthetic and it has been demonstrated that nasal chondrocytes (NC) provide for good cell yields and a high chondrogenic potential even post expansion [28-30]. Recently, NCs have shown to represent a promising autologous cell source for articular cartilage repair in several animal studies [31, 32] and may offer similar potential in IVD repair strategies [33].

The overall goal of this study was to develop an injectable self-assembled ECM hydrogel derived from native disc tissue and assess the effects of functionalised CS incorporation on the rheological properties and matrix forming capacity of nasal chondrocytes without growth factor supplementation.

2. Methods

2.1 ECM extraction, decellularisation and characterisation

Nucleus pulpous tissue was harvested from 18 month old bovine coccygeal discs under aseptic conditions. Discs were minced and treated with 20 ml/g of 200 mM sodium hydroxide (NaOH) at 4°C under constant rotation for 24h. NaOH treated fragments were then washed in diH_2O, freeze-dried and cryomilled (Spex SamplePrep 6770 Freezer/Mill) to obtain a fine powder. The decellularisation process was performed by adding 1 g of ECM powder to 50 ml of 50 mM Tris Buffer, 1 mM $MgCl_2$ solution supplemented with 2 U/ml of Benzonase® Nuclease (Merck Millipore, Ireland) and agitated at 37°C for 3 cycles of 1 hour each. Decellularisation solutions were changed at the end of each cycle. DNA content was determined using the quant-iT PicoGreen dsDNA Kit (Invitrogen) and base pair length was evaluated using agarose gel electrophoresis. Briefly, digests of decellularised ECM and native tissue as comparison were digested and purified using a Qiagen DNeasy® Blood and tissue extraction kit according to the manufacturer's instructions. Purified DNA samples were loaded into wells of 1% w/v agarose gel made with Tris Base-EDTA buffer and containing ethidium bromide. Gels were run at 80V for 60 minutes and imaged with a UV filter to detect DNA bands.

2.2 Functionalisation of chondroitin sulfate

Functionalisation of chondroitin sulfate (CS) was performed following a method previously described [9]. CS was dissolved in ultrapure water (UPW) containing 200 mM N-hydroxysuccinimide (NHS) and 200 mM 1-(3-dimethylaminopropyl)-3-ethylcarbodiimide hydrochloride (EDC) at a concentration of 50 mg/ml (molar ratio EDC:NHS:CS groups = 2.5:1.9:1.0). The pH of the solution was maintained at 4.75 and the reaction was allowed to proceed for 2 hours at room temperature and terminated by adjusting the pH of the solution to

7.4. The product of the reaction was dialysed against diH_2O at 4°C (MWCO 1kDa) and subsequently freeze-dried until further use.

2.3 Pre-gel fabrication

Decellularised NP ECM powder was solubilised at a concentration of 4% w/v in 0.5 M acetic acid solution supplemented with 2.5 mg/ml of pepsin (Sigma). Approximatively five bovine coccygeal discs were used to yield 20 ml of 4% solubilised ECM (sECM). sECM and functionalised CS (fCS) were mixed to obtain a final gel composition of 2% sECM-2% fCS (1:1 group), 2% sECM-1% fCS (1:0.5 group) for the initial study. Subsequently, only the 2% sECM-2% fCS composition was maintained (1:1 NHS+ group) and was compared to a 2% sECM-2% CS gel (1:1 NHS- group). A 2% sECM only gel was used as control (1:0) in both studies. The presence of salts in the pre-gel solutions was raised to physiological levels by adding 5% v/v 10x phosphate buffered saline (PBS) and pH was adjusted to 7.4 by adding small volumes of 4M NaOH.

2.4 Measuring degree of crosslinking using the TNBSA assay

The degree of crosslinking of CS to the primary amine groups of sECM was determined using the 2,4,6-trinitrobenzenesulfonic acid (TNBSA) assay as previously described [34, 35]. Briefly, after gelation had occurred, hydrogels were incubated in 0.1M sodium bicarbonate at pH 8.5. TNBSA (0.01%) was added to the samples and incubated for two hours at 37°C under constant agitation. Sodium dodecyl sulphate (SDS, 10%) and 1M hydrochloric acid (HCl) were used to terminate and stabilize the reaction. Samples were then incubated at 120°C for 15 minutes and the absorbance of each sample was read at a wavelength of 335 nm. The concentration of free amine groups was quantified by interpolation using a standard curve of known concentrations of glycine.

2.5 Hydrogel characterisation- Swelling ratio, degradation, elution kinetics and SEM imaging

Once gelation had occurred, initial weights of hydrogels were recorded, and samples were incubated in PBS at 37°C. At different time points (1, 3, 5 and 8 hours) samples were removed from PBS, their weight was recorded and incubated again at the same conditions. The swelling ratio was calculated as the ratio of the weight of the swollen sample at different time point to that of the initial hydrogel.

The resistance of different hydrogel compositions to enzymatic digestion was evaluated using a collagenase assay [34]. Briefly, hydrogels were incubated for 1 hour in 0.1 M Tris-HCl pH 7.4 containing 50 mM $CaCl_2$ at 37°C. Subsequently, 100 U/ml of collagenase type II (Gibco, Invitrogen, Dublin, Ireland), was added and samples were incubated at 37°C. Degradation buffer was sampled at different time points (1, 3 and 5 hrs) and stored at -20°C until biochemical analysis. Collagen content within the degradation buffer was quantified through the measurement of hydroxyproline content. Hydrogel degradation was expressed as a percentage of initial collagen detected in the sample.

Elution kinetics of CS from hydrogels was assessed under static and dynamic rotation conditions at 37°C. Briefly, after gelation, samples were transferred to 1 ml eppendorf tubes and 1 ml of PBS was added to each tube. In dynamic conditions, samples were maintained in agitation at 37°C using a rotator at 5 rpm (Stuart SB3, Cole-Parmer, UK). Native NP tissue biopsies served as a comparative control. Supernatants were assessed after 1, 3 and 6 hours and the sGAG content was determined using the diethylene blue dye binding assay. sGAG retention was calculated as a percentage of the initial sGAG content.

For SEM imaging, dehydrated samples were prepared by sputter coating with gold/palladium for 60s at a current of 40mA.

2.6 Rheological measurements and mechanical testing

Rheological measurements were performed with a MCR 102 rheometer (Anton-Paar, Hertford Herts, UK). In order to determine gelation kinetics, pre-gels with different sECM/fCS compositions were tested immediately after mixing. Storage moduli (G') and loss moduli (G'') were monitored as a function of time at a 10 Hz frequency and 1% strain at 37°C. The point of gelation of each pre-gel composition was identified as the crossing point between storage and loss moduli curves. After gelation had occurred, a frequency sweep analysis (0-100 Hz) was performed maintaining 1% strain at 37°C. Subsequently, the stress-realzation behavior of different gel compositions was studied by applying 10% constant strain and monitoring the relaxation over time at 37°C.

Mechanical testing was performed on hydrogels (Ø 6 mm x h 3 mm, n=3) in unconfined compression using a single column mechanical testing machine (Zwick/Roell Z2.5, Herefordshire, UK) and a 5 N load cell. Hydrogels were maintained in a PBS bath at room temperature. A preload of 0.01 N was applied for 30s to ensure that the surfaces of the hydrogel were in contact with the loading platens and subjected to 20% strain. Stress and strain data were recorded to calculate the Young's modulus.

The hydrogel mesh size ξ (m) was determined according to the Flory equation (1):

$$(1)\quad \xi = \sqrt[3]{(k_B T / G')}$$

With k_B representing the Boltzmann constant (J/K) and T the temperature (K) [36, 37]. The storage modulus G' is bound to the Young's modulus E by the relation (2):

$$(2)\ E = 2(1+\nu)G' = 3G'$$

where ν is Poisson's ratio and it is assumed to be the ideal value of 0.5, a reasonable approximation for a crosslinked gel [38]. Once combined, equations (1) and (2) define ξ as (3):

$$(3)\ \xi = \sqrt[3]{(3k_BT/E)}$$

2.7 Cell isolation and monolayer expansion

Porcine nasal tissue from five donors of up to six months of age was obtained from a local abattoir within 24 hours of sacrifice. Cells were isolated adopting a protocol previously developed in our lab [39]. Each experiment has been performed using cells isolated from three of the five donors. Septal cartilage was finely minced to ~2mm pieces and digested with 3000 U/ml of collagenase type II (Gibco, Invitrogen, Dublin, Ireland) in serum free Low Glucose–Dulbecco's Modified Eagle Medium (LG-DMEM) supplemented with penicillin (100 U/mL)–streptomycin (100 μg/ml) at a ratio of 10ml per gram of cartilage for 3 hours under constant rotation at 37°C. The digest was subjected to physical agitation using the Gentlemacs™ Tissue Dissociator (Milteny Biotech) and passed through a 40 μm cell strainer to separate cells from tissue debris and washed in LG-DMEM supplemented with penicillin (100 U/mL)–streptomycin (100 μg/ml) and 20% FBS. Cell yield and viability were determined with a haemocytometer and trypan blue exclusion. NCs were seeded at an initial density of $5x10^3$ cells/cm^2 in T-175 flasks and expanded to passage two (P2) in LG-DMEM supplemented with 10% FBS and 2% penicillin (100 U/mL)–streptomycin (100 μg/ml) in a humidified atmosphere at 37°C and 5% O_2.

2.8 Cell encapsulation, and culture

A suspension of monolayer expanded NCs was added to the pre-gel to obtain a final cell density of $1x10^6$ cells/ml. 80 μl of cell seeded pre-gel were cast using a 20g gauge needle syringe into cylindrical moulds of 6mm diameter and height of 3 mm, the moulds were submerged in LG-DMEM supplemented with 10% FBS and 2% penicillin (100 U/mL)–streptomycin (100 μg/ml) and incubated for 1 hour in a humidified atmosphere at 37°C and 5% O_2. After gelation, the

hydrogels were incubated for 14 days in a Chemically Defined Medium (CDM) consisting of LG-DMEM supplemented with 2% penicillin (100 U/mL)–streptomycin (100 μg/ml) , 0.25 μg/ml amphotericin B, 40 μg/ml L-proline, 1.5 mg/ml bovine serum albumin (BSA), 4.7 μg/ml linoleic acid, 1% insulin-transferrin-selenium, 50 μg/ml L-ascorbic acid-2-phosphate and 100 nM Dexamethasone (all from Sigma Aldrich). Media changes were performed twice weekly and conditioned media from changes was stored at 4^{o}C for biochemical assays. Hydrogels were assessed through biochemical and histological analyses at days 0 and 14. Gel contraction was assessed by measuring the change in diameter of hydrogels and is expressed as a percentage decrease at each time point relative to day 0.

2.9 Determination of DNA, sulphated glycosaminoglycan and collagen content

Samples were removed from fully supplemented CDM and stored at -80°C until further analysis. Samples were subsequently digested in 500 μl each of 100 mM sodium phosphate/5mM Na_2EDTA buffer containing 3.88 U/ml of papain enzyme and 5mM L-cysteine, pH 6.5 (all from Sigma-Aldrich) at 60°C under constant rotation for 12 hours. DNA content was quantified using the Hoechst Bisbenzimide 33258 dye assay (DNA QF Kit, Sigma-Aldrich). Sulfated glycosaminoglycan (sGAG) content was determined using the dimethylene blue dye binding assay. Total collagen content was quantified through the measurement of hydroxyproline content. Samples were hydrolysed at 110^{o}C in 38% HCl for 18 hours and assayed using a chloramine-T assay [40] and a hydroxyproline:collagen ratio of 1:7.69 [41]. Media obtained from media changes was also analysed for sGAG and collagen content.

2.10 Assessment of cell viability and morphology

Cell viability was assessed using a LIVE/DEAD® viability and cytotoxicity assay kit (Invitrogen). Samples were washed in PBS followed by a 1 hour incubation in phenol free LG-DMEM (Sigma-Aldrich, Dublin, Ireland) containing 4 μM Calcein AM and 4 μM Ethidium

Homodimer 1 (Cambridge Bioscience, Cambridge, UK). Samples were imaged with an Olympus FV-1000 Point-Scanning Confocal Microscope at 515 nm and 615 nm channels. Semi-quantitative analysis of cell viability and cell morphology were determined using IMAGEJ software (ImageJ, National Institute of Health, Bethesda, Maryland). In order to calculate a cell's circularity coefficient, the green channel was isolated from Live/Dead images and a mask was created to replace each cell with a "best fit" ellipse. Afterwards, circularity was calculated as the ratio between the shortest and the longest axis.

2.11 Histology and immunochemistry staining

Samples were removed from culture, washed in PBS and fixed in 4% paraformaldehyde (PFA) solution overnight at 4°C. Fixed samples were dehydrated and wax embedded. Sections (8 μm) were obtained with a microtome (Leica RM2125rt, Ashbourne, Ireland) and secured to microscope slides (Polylysine™, VWR, Dublin, Ireland). Sections were stained with 1% Alcian Blue 8GX in 0.1 M HCl to assess sGAG content. Collagen types I and II were evaluated using immunohistochemical techniques. Briefly, sections were treated with chondroitinase ABC (Sigma-Aldrich) in a humidified environment at 37°C, followed by incubation with 5% BSA to block non-specific sites. Next, collagen type I (Abcam 90395, 1:400) and collagen type II (Santa Cruz sc-52658, 1:400) primary antibodies (mouse monoclonal, IgG, Cambridge, UK) were applied overnight at 4°C, followed by 1 hour incubation with the secondary antibody (Anti-Mouse igG biotin conjugate, 1.5:200) (Sigma-Aldrich) and 45 minutes incubation with ABC reagent (Vectastain PK-400, Vector Labs, Peterborough, UK). Finally, sections were developed with DAB peroxidase (Vector Labs, Peterborough, UK) for 5 minutes.

2.12 Statistical analysis

Statistical analysis was performed using GraphPad Prism (version 7) software. One-way or Two-way ANOVA were used for analysis of variance. Results are displayed as mean ±

standard deviation, where N represents the number of biological donors or experiments performed and n represents the technical replicates for each respectively. Significance was accepted at a level of $p<0.5$.

3. Results

3.1 Decellularisation of ECM extracted from the NP

After completion of the treatment process from NP to ECM powder (Fig 1A), the material was decellularised and the effectiveness of the decellularisation process was assessed. Biochemical results demonstrated that the decellularisation procedure adopted successfully yielded a material whose DNA amount is below the decellularisation threshold of 50ng/mg [42] (Fig 1B). Moreover, the length of DNA base pairs remaining in the material post-decellularisation was less than 100 bp (Fig 1C). However, while efficiently removing DNA material and maintaining the amount of collagen present in native tissue (Fig 1D, E), the decellularisation process resulted in a 96% loss of sGAG when compared to native tissue (Fig 1E, F).

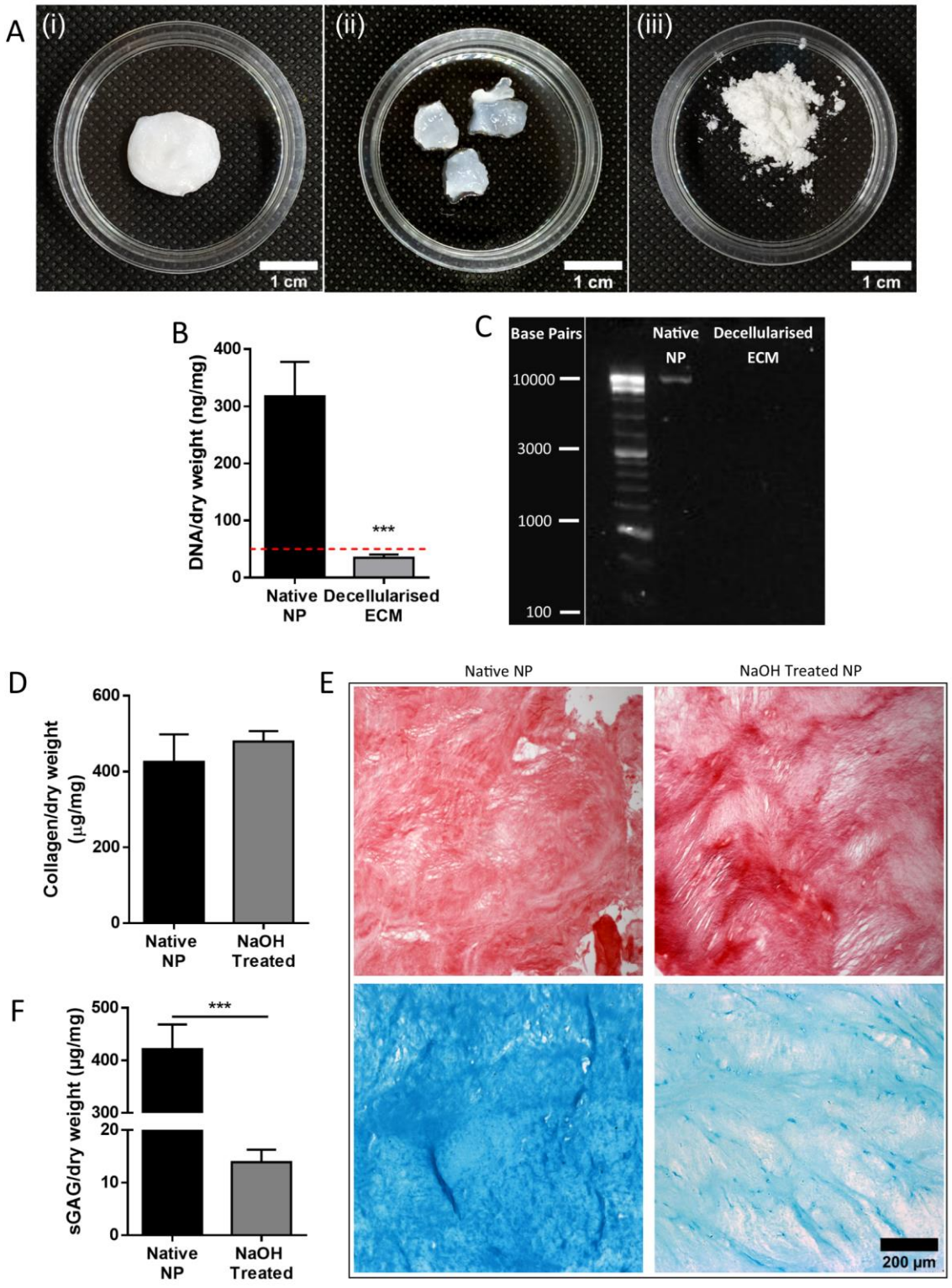

Figure 1 Decellularisation and characterisation (A) Freshly isolated caudal NP from bovine tail (i), NP appearance after NaOH treatment (ii), NP ECM powder after cryomilling (iii). (B) Quantification of DNA content in NP samples before and after the decellularisation process, *** indicates statistical significance $p<0.001$. Dashed red line indicates threshold of 50ng/mg.

(C) Base pair analysis. Agarose gel electrophoresis of DNA in NP tissue before and after decellularisation (DNA ladder 100 bp), (D) Collagen content in native NP and after NaOH treatment normalised by dry weight, (E) Collagen (top) and sGAG (bottom) histological evaluation of native and NaOh treated samples stained with picrosirius red and alcian blue respectively. (F) sGAG content in native NP and after NaOH treatment normalised by dry weight. *** indicates statistical significance $p<0.001$. N=1 donor, n=3 discs.

3.2 Incorporation of functionalised CS in gels improves their functional behaviour

Carboxyl activated or functionalised CS interacts with amine groups on collagen fibres to form a self-crosslinkable hydrogel system (Fig 2A). The effectiveness of crosslinking was assessed through the quantification of amine groups available on collagen fibres in sECM. The concentration of free amine groups available for crosslinking significantly decreases with the addition of fCS in a concentration dependent manner (Fig 2B). Higher amounts of fCS added resulted in decreased free amine groups. Swelling capacity was also found to increase with higher amounts of fCS (Fig 2C), with increased resistance to enzymatic degradation (Fig 2D). Gel contraction due to cellular activity was also found to decrease with fCS incorporation (82% in absence of CS; 47% for fCS containing gels), although no concentration dependence was observed (Fig 2E). fCS containing gels also exhibited different behaviors in response to fast ramp stress-relaxation tests (Fig 2F). The group containing the highest amount of fCS achieved a higher peak stress compared to the other groups, relaxed very rapidly at short times followed by a more gradual relaxation profile. Conversely, 1:0.5 and 1:0 groups exhibited a slower relaxation curve at all times. The results from the dynamic frequency sweep revealed that G' was always greater than G", indicating that each material adopted an elastic behavior in the range of the frequencies tested, regardless of the fCS content (Fig 2G). At higher frequencies the group containing the highest amount of fCS, yielded values of storage moduli that were significantly different than the other groups and comparable to values previously reported in

the literature for healthy NP tissue under similar testing conditions [43]. Moreover, the presence of higher concentrations of fCS in the gel composition resulted in shorter gelation times (Fig 2H, I).

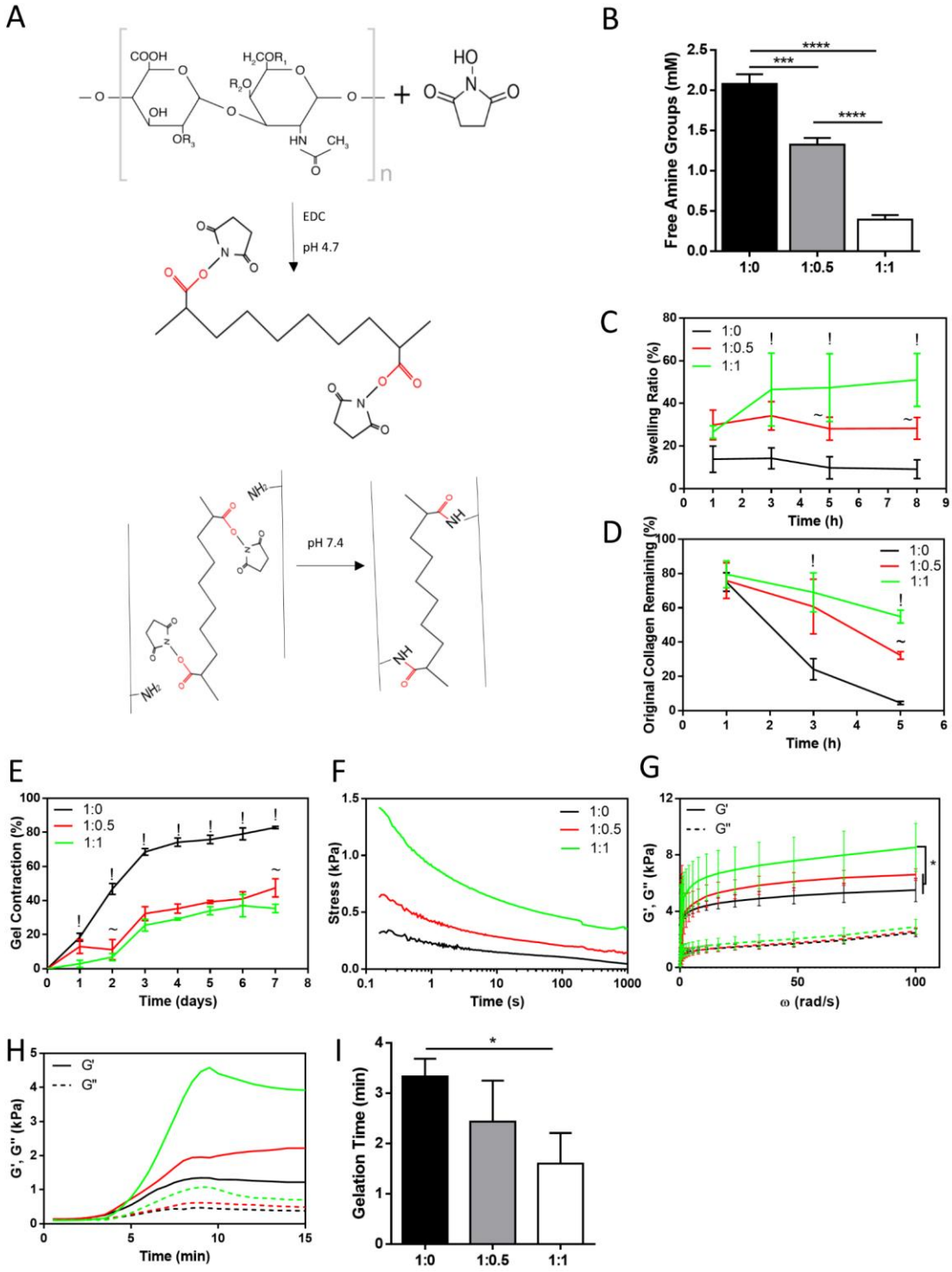

Figure 2 Gel characterisation. Solubilised ECM (sECM) and functionalised CS (fCS) were mixed to obtain the following gel compositions: 2% sECM-2% fCS (1:1), 2% sECM-1% fCS (1:0.5). A 2% sECM only gel was used as control (1:0). (A) Chondroitin sulfate functionalisation interacts with amine groups present on collagen during crosslinking to form self-assembled hydrogels. (B) Quantification of free amine groups post-crosslinking.

****($p<0.0001$), ***($p<0.001$). (C) Swelling profile of different compositions of ECM-CS gels. (D) Hydrogel enzymatic degradation kinetics. (E) Gel contraction kinetics for different composition of gels when seeded with nasal chondrocytes at a density of $1x10^6$ cells/ml for 7 days. ! ($p<0.05$) indicates statistical significance of all experimental groups compared with 1:0, ~ ($p<0.05$) indicates significance compared with 1:1 group. (F) Stress-Relaxation profile of 1:0, 1:0.5 and 1:1 groups. (G) Frequency sweep tests. (H) Storage (G') and Loss (G") Moduli curves observed during gelation at 37^{o}C, 10 Hz frequency and 1% strain. (I) Comparison of gelation times of hydrogels for different compositions. *($p<0.05$). N=1 donor, n=3 samples.

3.3 Synthesis of sGAG and collagen are dependent on the presence of CS in ECM hydrogels

Based on preliminary testing (data not shown), the highest amount of fCS that is possible to add to the material without compromising the structural integrity of the gels was found to be at a ratio of 1:1 (2% sECM-2% fCS). We next sought to determine the influence of the fCS-ECM hydrogel on NCs using this maximal concentration (1:1) compared to a lower fCS concentration (1:0.5), to ascertain if a lower amount is sufficient to promote enhanced cell activity, compared to a control without fCS (1:0). Gels were seeded with $1x10^6$ cell/ml and cultured in low oxygen (5% O_2) conditions in LG-DMEM for 14 days. A significant decrease in DNA content was measured at day 14 compared to day 0 in all groups examined, although no significant difference was observed among the different groups at the same time point (Fig 3A). Synthesis of sGAG was found to be dependent on the initial gel composition, with significantly more sGAG being deposited by cells in gels containing higher initial sGAG (Figure 3B, C). sGAG content at day 14 was calculated by subtracting sGAG content measured at day 0. Interestingly, collagen accumulation did not appear to be influenced by differences in the initial gel composition (Figure 3D, E). Finally, the sGAG/collagen ratio was found to increase linearly with increasing CS present in the initial gel composition (Fig 3F).

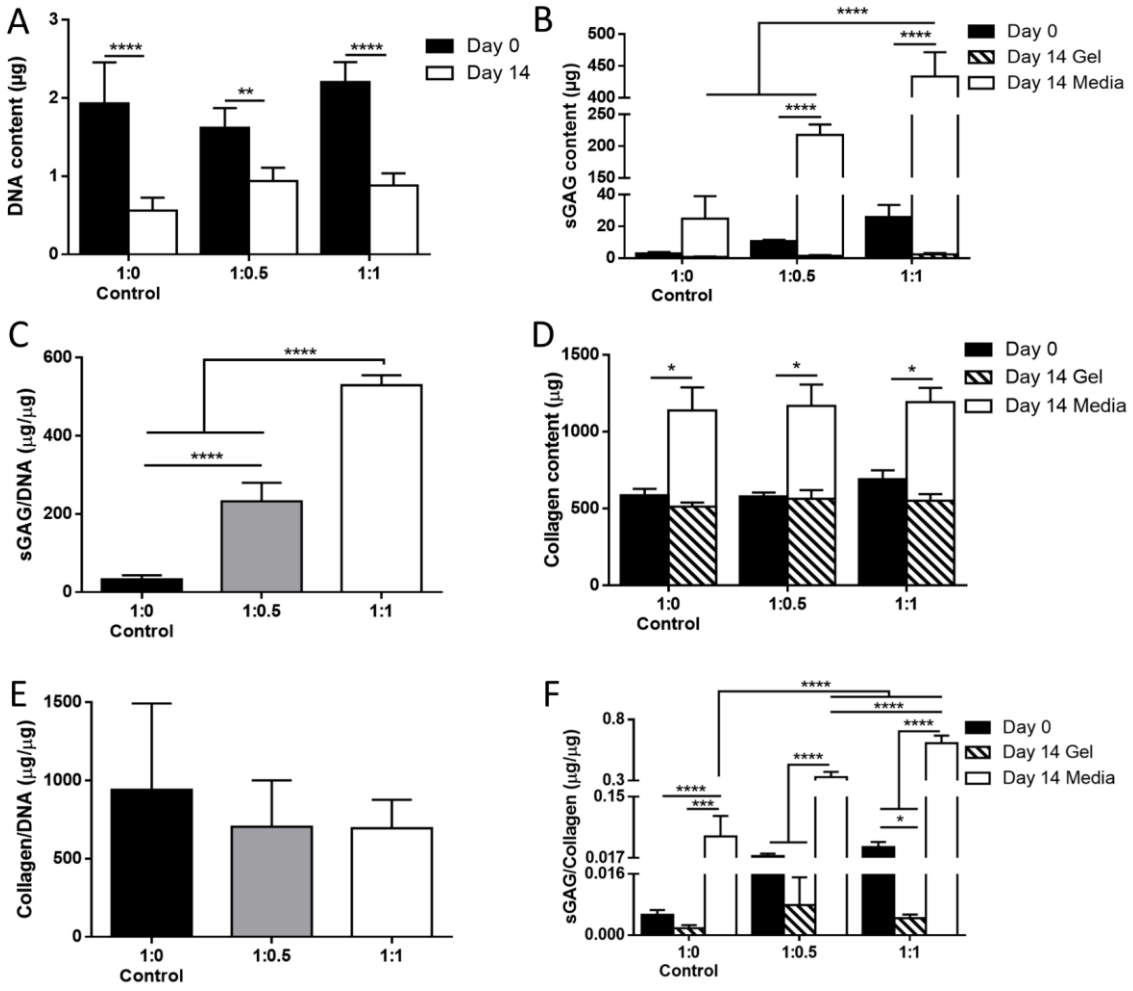

Figure 3 (A) DNA content in gels at Day 0 and Day 14. (B) Total sGAG accumulation after 14 days of culture. (C) sGAG produced over 14 days of culture normalised to DNA content. sGAG produced was determined as the difference between the total amount of sGAG detected at day 14 and day 0 (D) Collagen content in day 0 gels and total collagen retained in gels at day 14 and in culture media. (E) Collagen produced over 14 days of culture normalised to DNA content. Collagen production was calculated by subtracting collagen content at day 0 from day 14. (F) sGAG:Collagen ratio. The value was calculated as a ratio between sGAGs and collagen produced during the culture period. N=3 donors, n=3 samples.

3.4 The presence of CS in the gel composition positively influences cell morphology

Motivated by previous results demonstrating a higher sGAG/collagen ratio for the gel composition of sECM:fCS of 1:1, it was decided to examine in more detail the effects of CS incorporation in sECM gels at this ratio. In order to determine the effect of CS functionalisation on cell behaviour, CS was incorporated into gels either in a functionalised (NHS+) or non-functionalised (NHS-) form and compared to sECM only controls. The presence of CS, both functionalised or non-functionalised, was found to positively influence the morphology of NCs inhibiting spreading and favouring the adoption of a rounded cell shape (Figure 4A-C). Semi-quantitative analysis of cell circularity corroborated these observations, demonstrating a correlation between the presence of CS and a rounded cell morphology, with a significant difference between sECM control and NHS+ group after 14 days of culture (Fig 4D). Live/Dead analysis revealed similar viability levels (~85%) for all formulations (Fig 4E). Interestingly, a decrease in DNA content was observed at day 14, although DNA content in NHS+ was found to be higher on day 14 compared to the control group (Fig 4F).

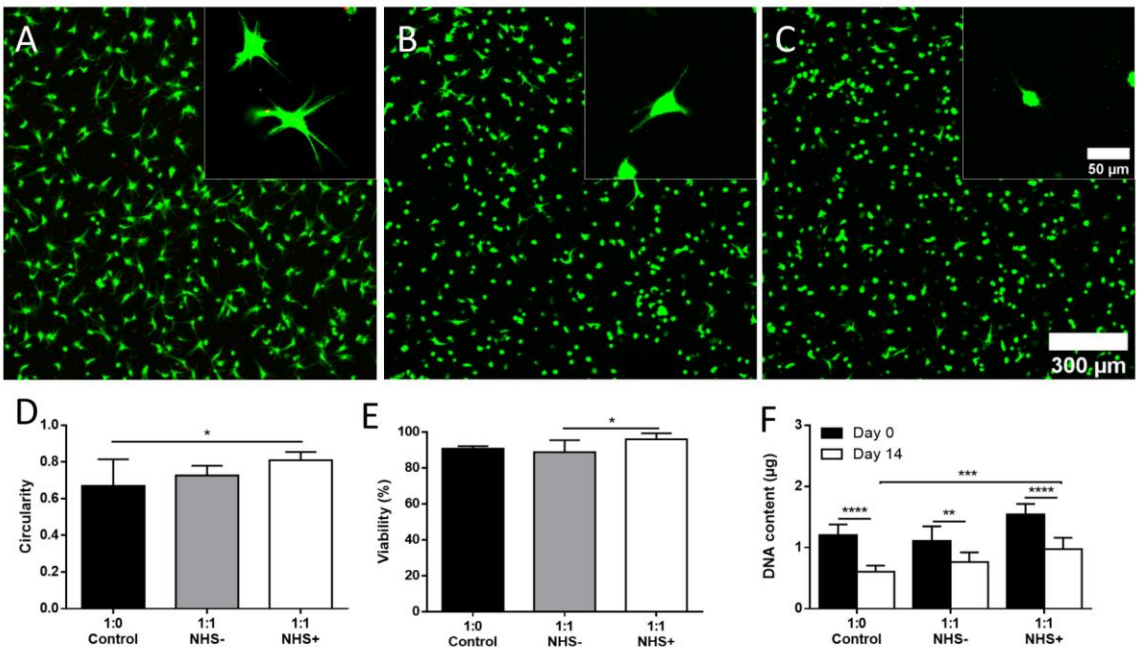

Figure 4 Live/Dead imaging at day 14 of nasal chondrocytes in sECM (no CS) hydrogels (A), NHS- gels (B), and in NHS+ gels (scale bar is 300µm) (C) with cell morphology (inset; scale

bar is 50μm) for the different gel compositions. (D) Semi-quantitative analysis of cell circularity. (E) Semi-quantitative analysis of cell viability (%). (F) DNA content at Day 0 and Day 14. N=3 donors, n=3 samples.

3.5 CS incorporation is essential to promote sGAG and collagen matrix deposition

When compared to cells in the control group, NCs cultured in CS containing gels produced significantly higher amounts of sGAG (Fig 5A), the totality of which, however, was detected in the culture media. Similar results were observed on a per cell basis when normalising sGAG per DNA content (Fig 5B). Interestingly, when normalised by DNA content, NHS- gels yielded higher sGAG synthesis compared to NHS+ functionalised hydrogels. Histological staining demonstrated intense deposition of sGAG in the pericellular region of NCs cultured in CS containing gels at day 14, while no appreciable sGAG deposition was visible in the control group at the same time point (Fig 5C).

In terms of collagen content, NCs cultured in CS supplemented gels exhibited a reduced content at day 14 in comparison with NCs in control gels (no CS) (Fig 6A), with similar trends observed when normalised on a per cell basis (Fig 6B). Finally, both the CS containing gels showed a significantly higher sGAG/collagen ratio than controls, the highest being the NHS- gels (Fig 6C). Interestingly, immunohistochemical analysis revealed intense collagen type 2 and weak collagen type 1 staining in CS containing gels, while an opposite pattern was found for gels in the control group with more collagen type I being deposited compared to collagen type II (Fig 6D).

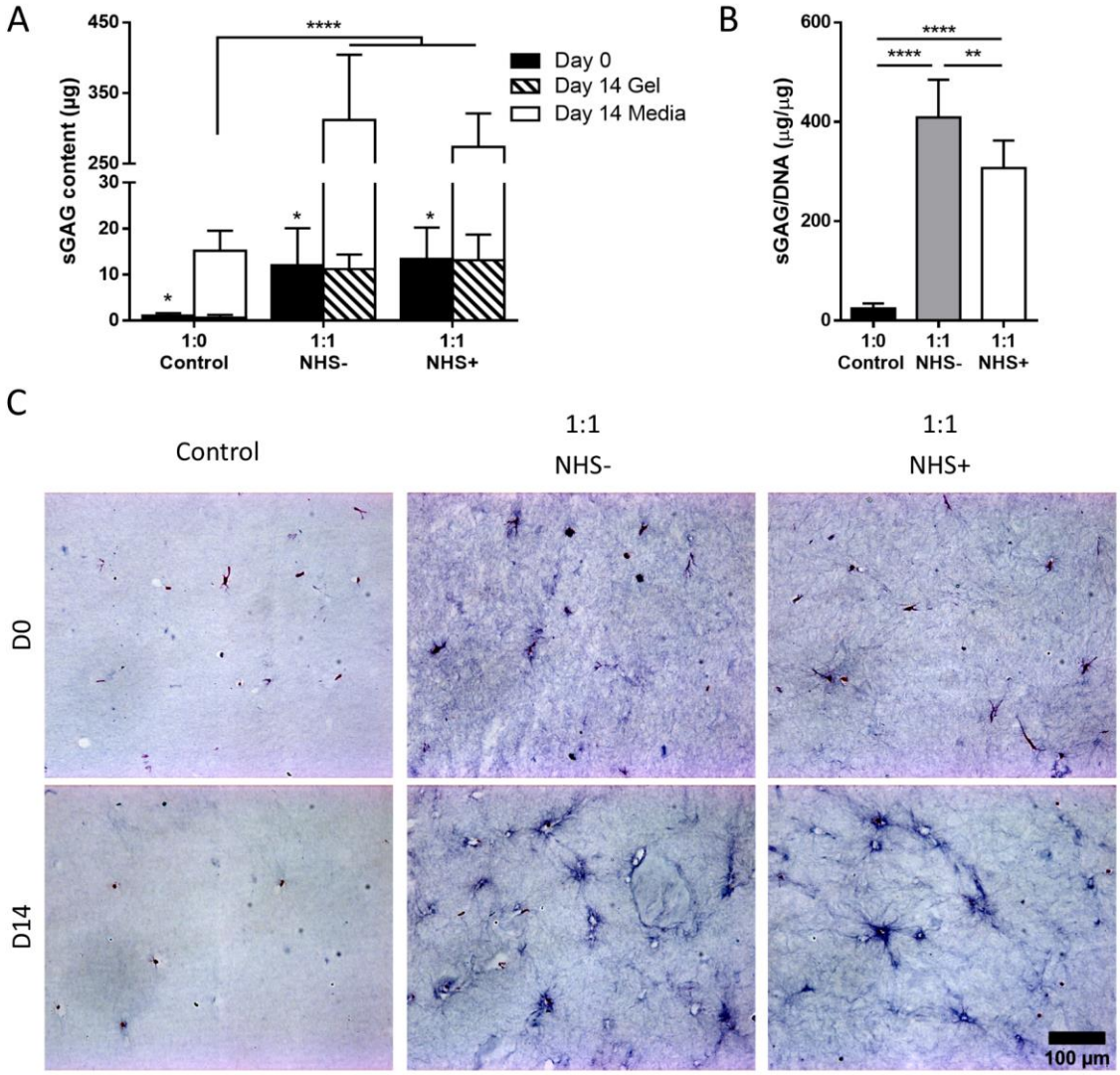

Figure 5 (A) sGAG content at day 0 and day 14. Day 14 measurements have been represented as sGAG released in the media and sGAG retained in the gels. (B) sGAG produced over 14 days of culture normalised to DNA content. sGAG produced was determined as the difference between the total amount of sGAG detected at day 14 and day 0. N=3 donors, n=3 samples. (C) sGAG histological evaluation with alcian blue/nuclear fast red at day 0 and day 14. Scale bar is 100µm

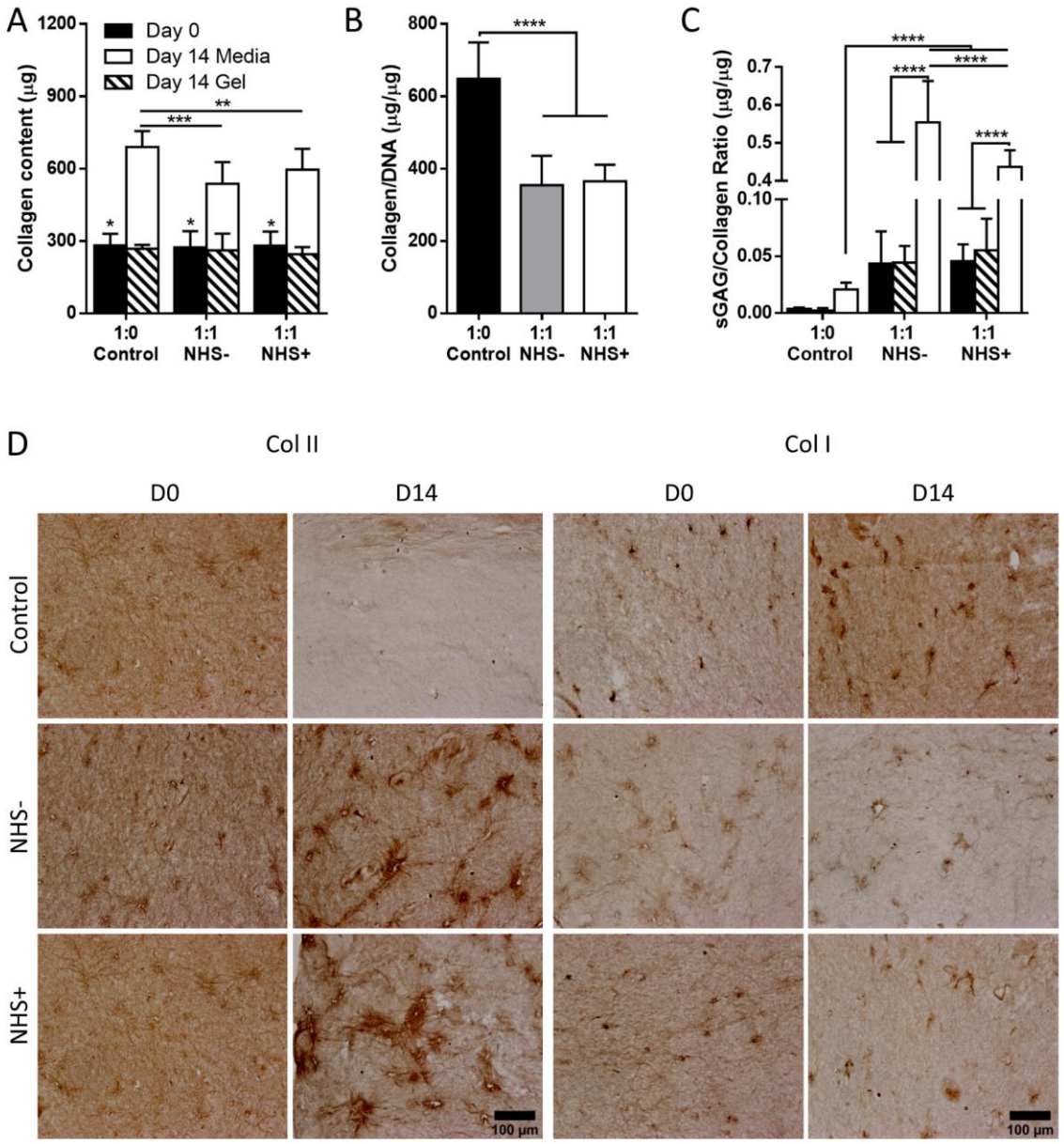

Figure 6 (A) Collagen content in day 0 gels and total collagen retained in gels at day 14 and in the culture media. (B) Collagen produced over 14 days of culture normalised to DNA content. Collagen production was calculated by subtracting collagen content at day 0 from day 14 (Media+Gel). (C) sGAG:Collagen ratio. The value was calculated as the ratio between sGAGs and collagen produced during the culture period. N=3 donors, n=3 samples. (D) Immunohistochemical staining for collagen type 2 and collagen type 1. Scale bar is 100µm.

3.6 Functionalisation of CS improves mechanical integrity and sGAG retention of hydrogels

Mechanical integrity and stability of gels was assessed optically by comparing the degree of shape maintenance upon gelation after 10 minutes of free standing. As showed in Fig 7A, NHS- gels were unable to maintain structural stability, in contrast with control and NHS+ gels. Moreover, the elastic modulus of the three groups of gels was determined, with NHS+ gels exhibiting a significantly higher modulus compared to both NHS- and control gels (Fig 7B). Furthermore, the elastic modulus of NHS+ gels was found to be comparable to the values previously reported in literature for native bovine NP [44, 45], but still lower than native human NP [46-48]. To further characterise the hydrogels based on their composition, the average mesh size (ξ), corresponding to the average distance between crosslinks in the hydrogel network, was determined using equation (3). The analysis revealed a mesh size of 267.4±26.9 nm in NHS+ gels, 842.9±310.2 nm in NHS- gels, and 522.5±53.7 nm in the control group. sGAG retention was determined under dynamic and static conditions and compared to native NP. After 6 hours of dynamic agitation CS present in NHS- gels had been completely depleted, while NHS+, had retained 50% of the initial GAG content similar to native NP tissue (Fig 7C). Under static conditions, NHS+ gels retained higher levels of sGAG (>40%) when compared to NHS- gels (Fig 7D).

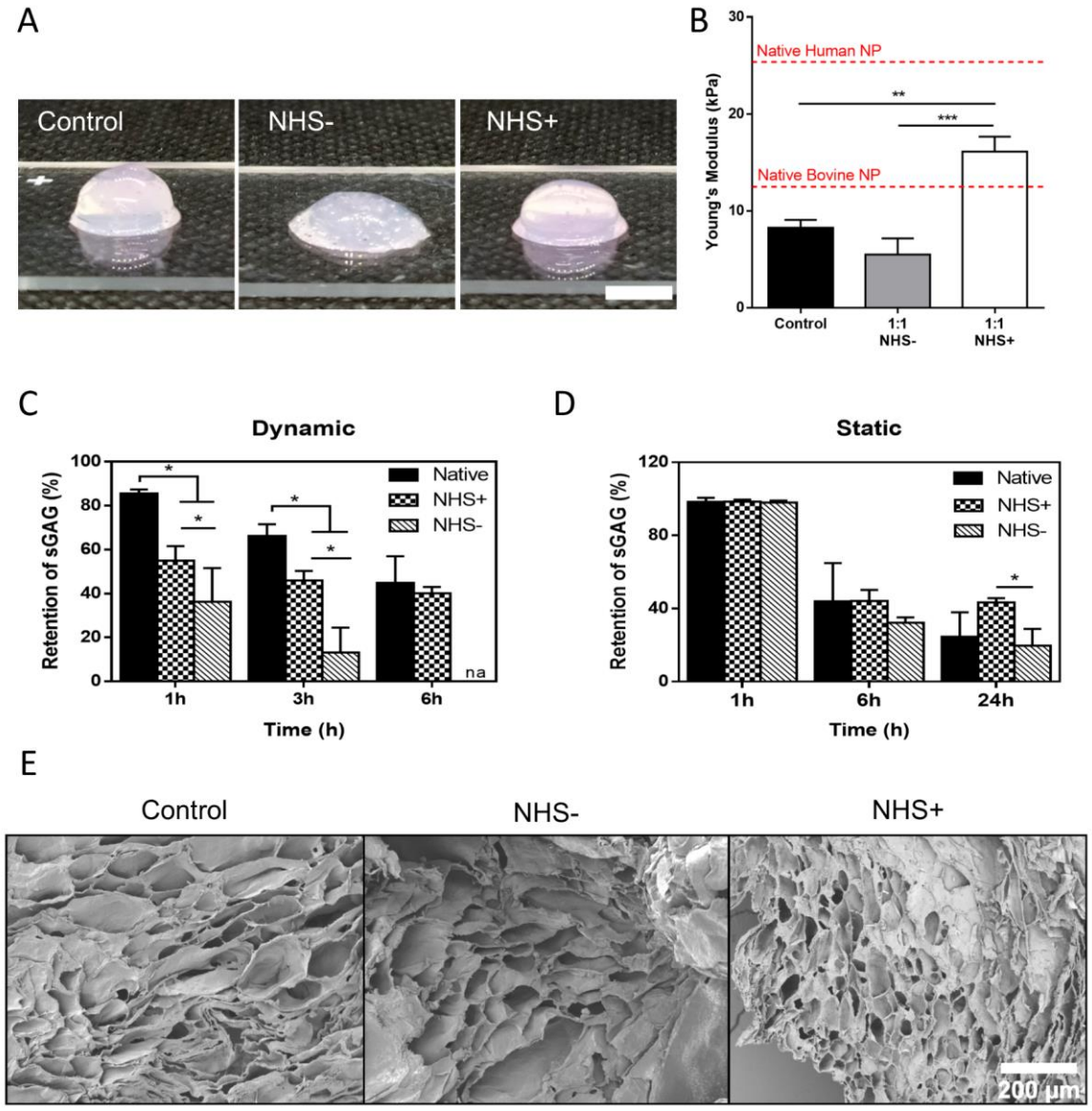

Figure 7 (A) Assessment of the structural stability of cell free ECM-derived hydrogels post gelation after 10 minutes of free standing. Scale bar is 5 mm (B) Young's modulus. (C) Retention of sGAGs in hydrogels subjected to dynamic agitation and (D) static conditions. n=3 samples. (E) SEM images of Control, NHS- and NHS+ samples. Scale bar is 200 µm.

4. Discussion

The goal of this study was to develop an injectable and self-assembled biomimetic tissue derived material and to evaluate its potential as a biomaterial for promoting nucleus pulposus

regeneration. Although the use of decellularised tissue specific ECM has been widely investigated for a variety of tissue engineering (TE) applications [14, 15, 17, 49-52], decellularisation and solubilisation techniques inevitably result in significant loss of the sGAG [15, 17, 53, 54]. In an attempt to reincorporate sGAG to enhance bioactivity and overcome the challenges with poor gelation in a carbohydrate rich environment, we successfully functionalised CS as a crosslinker to restore the material's biomimetic and structural characteristics. In the functionalisation process we allowed EDC to react with the carboxyl groups of CS forming an unstable amine-reactive ester intermediate, which was then stabilised with the addition of NHS. This functionalisation strategy has been previously adopted for different tissue engineering applications. Cao et al. used this chemistry to develop collagen type II-chondroitin sulfate scaffolds for cartilage regeneration [55], while Lai et al. applied it in the preparation of gelatin-chondroitin sulfate scaffolds for corneal regeneration [56], both showing improved biosynthetic ability and morphology retention for articular chondrocytes and keratocytes respectively. More recently, Gao et al. have investigated the physical properties of commercial collagen type II-chondroitin sulfate hydrogels and showed that they were able to support survival and proliferation of encapsulated articular chondrocytes [27]. Through the addition of fCS to the gel composition, we enhanced desirable characteristics of the hydrogels such as high swelling capacity and short gelation time, allowing the functionalised biomaterial to be able to hold 4 times as much water and gel twice as fast compared to sECM hydrogels. One approach for the treatment of DD that has been commercially available for the past ten years, comprises of the injection of in vitro expanded autologous disc cells into the degenerated disc [57]. Although the study showed promising results, significant concerns have been raised in regards of cell leakage via the needle tract post-delivery [58, 59]. The use of a fast-gelling material such as the one presented in this work could allow cells to be immobilised in situ in a

shorter time frame and avoid leakage while simultaneously ensuring better hydration than an ECM only material.

Ideally, CS should be added to the gel composition in the same proportion as the native NP [60]. However, gel formulations with fCS:sECM ratios higher than 1 systematically failed to maintain structural stability (data not shown). The effect of CS supplementation on metabolism and differentiation has already been observed for mesenchymal stem cells (MSCs) [20, 61, 62] and articular chondrocytes (AC) [19, 63-67] for cartilage regeneration applications, however, there is little knowledge about its effect on NCs. In the first part of this study we evaluated how different gel compositions influence NC behaviour with respect to matrix deposition and found that supplementation with CS elevated the levels of matrix sGAG production. This result is consistent with previous studies reporting that CS supplementation can improve matrix accumulation for cells in either 2D or 3D culture [19, 62, 63, 65-67]. In line with our expectations, we found that the increase in sGAG production is dependent on gel composition, with a higher ratio of sGAG/Collagen being synthetized by NCs in gels prepared with higher amounts of fCS. However, although the presence of CS in the gel composition enhanced sGAG production with a sGAG/Collagen ratio comparable to the native bovine NP (typically ranging from 1:1 to 2:1), the ratio was still lower than the native human NP, which is typically 3.5:1 [3, 60].

Chondrocytes are well-known to be phenotypically unstable and undergo de-differentiation when expanded in 2D monolayer or cultured in 3D collagen scaffolds or hydrogels [68-70]. The transition from chondrocytic to a fibroblastic phenotype has been shown to occur with a dramatic change in cell shape and metabolism, and with a marked production of fibro-cartilaginous tissue, suggesting a possible relation between the two. The correlation between cell morphology and differentiation state has been under intense investigation in the past decades [71-73]. The presence of CS (functionalised and non-functionalised) was observed to

promote a rounded cell morphology, while cells exhibited a more spread-like morphology for ECM only gels. The result suggests that the presence of CS in the cell microenvironment plays an active role in modelling its spatial conformation. There are a number of ways in which a matrix macromolecule such as CS can physiologically affect a cell: it can act as a physical barrier between the cell and the attachment sites available on the collagen structure, or act as a chemical barrier regulating ion exchanges to and from the cell [74]. It has recently been shown that GAGs can bind and sequester a wide range of proteins, the most interesting of which are the families of growth factors (GF) and cytokines. By binding these small signalling molecules, GAGs indirectly regulate cell activity by either acting as co-factor and become readily available to the cell receptor, or by limiting their availability to the cell [75, 76]. The presence of CS in the cell microenvironment could therefore serve as a reservoir for cytokines and GFs to aid cell-cell communications, which could possibly help maintain their differentiated state.

In contrast with results from previous studies [66, 67], the presence of CS or fCS did not have a major impact on cell viability. However, conflicting results from similar studies showed no change in cell proliferation and viability when exposed to CS, suggesting that there is still no consensus regarding the impact of sGAG on cell survival [19, 63, 65]. In our study we observed a decrease in the DNA levels at the end of the culture in every group, suggesting significant cell death. However, the high viability observed from Live/Dead staining at the same time point suggests that cells could have simply leaked out of the gels thereby reducing overall DNA content. This could be due to the characteristic typical of type II collagen, the main component of sECM, of forming fibre networks perhaps too loose to guarantee high cell retention during in vitro culture.

Interestingly, we found that CS supplementation, regardless of NHS functionalisation, was capable of enhancing sGAG production compared to ECM only gels while at the same time inhibiting collagen deposition in the absence of growth factor stimulation. Immunohistological

analysis revealed a substantial difference in the type of collagen deposited in the pericellular region, with collagen type II being predominantly deposited in CS supplemented gels and collagen type I in ECM only gels. Differentiated chondrocytes typically produce two structural macromolecules, cartilage-specific proteoglycans and collagen type II. The transition from the synthesis of one type of collagen to another is widely known to be highly indicative of the chondrocytes' differentiation state [77-79]. Taken together, the results suggest that the addition of CS to a native sECM gel facilitates NCs in culture to maintain a differentiated phenotype, resulting in the deposition of the appropriate and specific ECM.

The correlation between the presence of GAGs in solution and the ability of collagen to form fibrillar reticulates has been investigated extensively over the years [23, 25, 80, 81] demonstrating that collagen gel structures are considerably weaker when formed in the presence of GAGs. Stuart and Panitch showed in particular how fibrillogenesis in the presence of CS in a physiological environment resulted in an increase in void spaces for a collagen type I network, which yielded a reduced stiffness [81]. Interestingly, further investigations on the mechanical properties of our gel compositions revealed that when CS is supplemented without any functionalisation (NHS-) the resulting gel lacks structural stability and integrity. Another key desired characteristic is the ability to retain the incorporated sGAG. Retention kinetics demonstrated that fCS formulations were better suited to this aim and elution kinetics and mechanical properties were found to be comparable to native tissue, and superior to non-functionalised CS hydrogels. Overall, these findings suggest that the addition of CS in the sECM base hydrogel promotes the retention of a differentiated phenotype for NCs with concomitant specific ECM deposition, and that CS functionalisation is necessary to ensure adequate structural integrity. Preliminary in vitro culture experiments performed in our laboratory using NP cells and the fCS ECM biomaterial (data not shown), did not reveal any

deleterious or negative effects in terms of cell viability or in matrix production. This is important as any injected material will come in contact with resident NP cells.

5. Conclusion

In this work we have successfully developed an injectable self-assembled biomimetic biomaterial combining decellularised and solubilised ECM from bovine NP tissue and functionalised CS. The inclusion of CS in the composition of the material appears to be critical for promoting a rounded cell morphology and subsequent deposition of NP-like matrix. However, some limitations should be noted. In this study we have focused on the synthesis of sGAG as an indicator of NP-like matrix production. However, it would be important to also determine whether synthesised sGAG are integrated within a proteoglycan to reduce the likelihood that they could easily diffuse out of the organ after being synthesised. Moreover, animal studies are an important aspect for clinical translation and warrant further investigation. Taken together, the results of this study show the potential benefit of using the proposed biomaterial in conjunction with NCs to support the regeneration of NP tissue

Funding

This work was supported by Science Foundation Ireland Career Development Award (15/CDA/3476).

References

[1] H.S. An, E.J. Thonar, K. Masuda, Biological repair of intervertebral disc, Spine (Phila Pa 1976) 28(15 Suppl) (2003) S86-92.

[2] W.M. Erwin, L. DeSouza, M. Funabashi, G. Kawchuk, M.Z. Karim, S. Kim, S. Mdler, A. Matta, X. Wang, K.A. Mehrkens, The biological basis of degenerative disc disease: proteomic and biomechanical analysis of the canine intervertebral disc, Arthritis Res Ther 17 (2015) 240.
[3] P.J. Roughley, Biology of intervertebral disc aging and degeneration: involvement of the extracellular matrix, Spine (Phila Pa 1976) 29(23) (2004) 2691-9.
[4] B.R. Whatley, X.J. Wen, Intervertebral disc (IVD): Structure, degeneration, repair and regeneration, Mat Sci Eng C-Mater 32(2) (2012) 61-77.
[5] M. Barandun, L.D. Iselin, F. Santini, M. Pansini, C. Scotti, D. Baumhoer, O. Bieri, U. Studler, D. Wirz, M. Haug, M. Jakob, D.J. Schaefer, I. Martin, A. Barbero, Generation and characterization of osteochondral grafts with human nasal chondrocytes, J Orthop Res 33(8) (2015) 1111-9.
[6] S.S. Sivan, A.J. Hayes, E. Wachtel, B. Caterson, Y. Merkher, A. Maroudas, S. Brown, S. Roberts, Biochemical composition and turnover of the extracellular matrix of the normal and degenerate intervertebral disc, Eur Spine J 23 Suppl 3 (2014) S344-53.
[7] S.P. Hughes, A.J. Freemont, D.W. Hukins, A.H. McGregor, S. Roberts, The pathogenesis of degeneration of the intervertebral disc and emerging therapies in the management of back pain, J Bone Joint Surg Br 94(10) (2012) 1298-304.
[8] J.A. Buckwalter, A. Pedrini-Mille, V. Pedrini, C. Tudisco, Proteoglycans of human infant intervertebral disc. Electron microscopic and biochemical studies, J Bone Joint Surg Am 67(2) (1985) 284-94.
[9] J.S. Kwon, S.M. Yoon, S.W. Shim, J.H. Park, K.J. Min, H.J. Oh, J.H. Kim, Y.J. Kim, J.J. Yoon, B.H. Choi, M.S. Kim, Injectable extracellular matrix hydrogel developed using porcine articular cartilage, Int J Pharm 454(1) (2013) 183-91.
[10] J. Wu, Q. Ding, A. Dutta, Y. Wang, Y.H. Huang, H. Weng, L. Tang, Y. Hong, An injectable extracellular matrix derived hydrogel for meniscus repair and regeneration, Acta Biomater 16 (2015) 49-59.
[11] S. Romanazzo, S. Vedicherla, C. Moran, D.J. Kelly, Meniscus ECM-functionalised hydrogels containing infrapatellar fat pad-derived stem cells for bioprinting of regionally defined meniscal tissue, J Tissue Eng Regen Med 12(3) (2018) e1826-e1835.
[12] O.A. Burnsed, Z. Schwartz, K.O. Marchand, S.L. Hyzy, R. Olivares-Navarrete, B.D. Boyan, Hydrogels derived from cartilage matrices promote induction of human mesenchymal stem cell chondrogenic differentiation, Acta Biomater 43 (2016) 139-149.
[13] J.L. Zou, S. Liu, J.H. Sun, W.H. Yang, Y.W. Xu, Z.L. Rao, B. Jiang, Q.T. Zhu, X.L. Liu, J.L. Wu, C. Chang, H.Q. Mao, E.A. Ling, D.P. Quan, Y.S. Zeng, Peripheral Nerve-Derived Matrix Hydrogel Promotes Remyelination and Inhibits Synapse Formation, Adv Funct Mater 28(13) (2018).
[14] G.M. Cunniffe, P.J. Diaz-Payno, J.S. Ramey, O.R. Mahon, A. Dunne, E.M. Thompson, F.J. O'Brien, D.J. Kelly, Growth plate extracellular matrix-derived scaffolds for large bone defect healing, Eur Cell Mater 33 (2017) 130-142.
[15] C. Fernandez, A. Marionneaux, S. Gill, J. Mercuri, Biomimetic nucleus pulposus scaffold created from bovine caudal intervertebral disc tissue utilizing an optimal decellularization procedure, J Biomed Mater Res A 104(12) (2016) 3093-3106.
[16] J.J. Mercuri, S. Patnaik, G. Dion, S.S. Gill, J. Liao, D.T. Simionescu, Regenerative potential of decellularized porcine nucleus pulposus hydrogel scaffolds: stem cell differentiation, matrix remodeling, and biocompatibility studies, Tissue Eng Part A 19(7-8) (2013) 952-66.
[17] S. Illien-Junger, D.D. Sedaghatpour, D.M. Laudier, A.C. Hecht, S.A. Qureshi, J.C. Iatridis, Development of a bovine decellularized extracellular matrix-biomaterial for nucleus pulposus regeneration, Journal of Orthopaedic Research 34(5) (2016) 876-888.
[18] H. Lin, G. Yang, J. Tan, R.S. Tuan, Influence of decellularized matrix derived from human mesenchymal stem cells on their proliferation, migration and multi-lineage differentiation potential, Biomaterials 33(18) (2012) 4480-9.
[19] C.T. Bassleer, J.P. Combal, S. Bougaret, M. Malaise, Effects of chondroitin sulfate and interleukin-1 beta on human articular chondrocytes cultivated in clusters, Osteoarthritis Cartilage 6(3) (1998) 196-204.

[20] S. Varghese, N.S. Hwang, A.C. Canver, P. Theprungsirikul, D.W. Lin, J. Elisseeff, Chondroitin sulfate based niches for chondrogenic differentiation of mesenchymal stem cells, Matrix Biol 27(1) (2008) 12-21.
[21] L. Tio, C. Orellana, S. Perez-Garcia, L. Piqueras, P. Escudero, Y. Juarranz, N. Garcia-Giralt, F. Montanes, A. Farran, P. Benito, R.P. Gomariz, M.J. Sanz, J. Monfort, Effect of chondroitin sulphate on synovitis of knee osteoarthritic patients, Med Clin (Barc) 149(1) (2017) 9-16.
[22] C. Li, K. Wang, X. Zhou, T. Li, Y. Xu, L. Qiang, M. Peng, Y. Xu, L. Xie, C. He, B. Wang, J. Wang, Controllable fabrication of hydroxybutyl chitosan/oxidized chondroitin sulfate hydrogels by 3D bioprinting technique for cartilage tissue engineering, Biomed Mater 14(2) (2019) 025006.
[23] B.P. Toole, D.A. Lowther, The effect of chondroitin sulphate-protein on the formation of collagen fibrils in vitro, Biochem J 109(5) (1968) 857-66.
[24] P.N. Lewis, C. Pinali, R.D. Young, K.M. Meek, A.J. Quantock, C. Knupp, Structural interactions between collagen and proteoglycans are elucidated by three-dimensional electron tomography of bovine cornea, Structure 18(2) (2010) 239-45.
[25] C. Ruhland, E. Schonherr, H. Robenek, U. Hansen, R.V. Iozzo, P. Bruckner, D.G. Seidler, The glycosaminoglycan chain of decorin plays an important role in collagen fibril formation at the early stages of fibrillogenesis, FEBS J 274(16) (2007) 4246-55.
[26] J.H. Shepherd, S. Ghose, S.J. Kew, A. Moavenian, S.M. Best, R.E. Cameron, Effect of fiber crosslinking on collagen-fiber reinforced collagen-chondroitin-6-sulfate materials for regenerating load-bearing soft tissues, J Biomed Mater Res A 101(1) (2013) 176-84.
[27] Y. Gao, B. Li, W. Kong, L. Yuan, L. Guo, C. Li, H. Fan, Y. Fan, X. Zhang, Injectable and self-crosslinkable hydrogels based on collagen type II and activated chondroitin sulfate for cell delivery, Int J Biol Macromol 118(Pt B) (2018) 2014-2020.
[28] W. Kafienah, M. Jakob, O. Demarteau, A. Frazer, M.D. Barker, I. Martin, A.P. Hollander, Three-dimensional tissue engineering of hyaline cartilage: comparison of adult nasal and articular chondrocytes, Tissue Eng 8(5) (2002) 817-26.
[29] J.H. Henderson, J.F. Welter, J.M. Mansour, C. Niyibizi, A.I. Caplan, J.E. Dennis, Cartilage tissue engineering for laryngotracheal reconstruction: comparison of chondrocytes from three anatomic locations in the rabbit, Tissue Eng 13(4) (2007) 843-53.
[30] A.G. Tay, J. Farhadi, R. Suetterlin, G. Pierer, M. Heberer, I. Martin, Cell yield, proliferation, and postexpansion differentiation capacity of human ear, nasal, and rib chondrocytes, Tissue Eng 10(5-6) (2004) 762-70.
[31] W. Chen, C. Li, M. Peng, B. Xie, L. Zhang, X. Tang, Autologous nasal chondrocytes delivered by injectable hydrogel for in vivo articular cartilage regeneration, Cell Tissue Bank 19(1) (2018) 35-46.
[32] M. Mumme, A. Barbero, S. Miot, A. Wixmerten, S. Feliciano, F. Wolf, A.M. Asnaghi, D. Baumhoer, O. Bieri, M. Kretzschmar, G. Pagenstert, M. Haug, D.J. Schaefer, I. Martin, M. Jakob, Nasal chondrocyte-based engineered autologous cartilage tissue for repair of articular cartilage defects: an observational first-in-human trial, Lancet 388(10055) (2016) 1985-1994.
[33] S. Vedicherla, C.T. Buckley, In vitro extracellular matrix accumulation of nasal and articular chondrocytes for intervertebral disc repair, Tissue Cell 49(4) (2017) 503-513.
[34] M. Monaghan, S. Browne, K. Schenke-Layland, A. Pandit, A collagen-based scaffold delivering exogenous microrna-29B to modulate extracellular matrix remodeling, Mol Ther 22(4) (2014) 786-96.
[35] Y. Garcia, R. Collighan, M. Griffin, A. Pandit, Assessment of cell viability in a three-dimensional enzymatically cross-linked collagen scaffold, J Mater Sci Mater Med 18(10) (2007) 1991-2001.
[36] F. Nativel, D. Renard, F. Hached, P.G. Pinta, C. D'Arros, P. Weiss, C. Le Visage, J. Guicheux, A. Billon-Chabaud, G. Grimandi, Application of Millifluidics to Encapsulate and Support Viable Human Mesenchymal Stem Cells in a Polysaccharide Hydrogel, Int J Mol Sci 19(7) (2018).
[37] F. Flory, Principles of Polymer Chemistry, Ithaca, NY, USA, 1953.
[38] D.L. Elbert, J.A. Hubbell, Conjugate addition reactions combined with free-radical cross-linking for the design of materials for tissue engineering, Biomacromolecules 2(2) (2001) 430-41.

[39] S. Vedicherla, C.T. Buckley, Rapid Chondrocyte Isolation for Tissue Engineering Applications: The Effect of Enzyme Concentration and Temporal Exposure on the Matrix Forming Capacity of Nasal Derived Chondrocytes, Biomed Res Int 2017 (2017) 2395138.
[40] W. Kafienah, T.J. Sims, Biochemical methods for the analysis of tissue-engineered cartilage, Methods Mol Biol 238 (2004) 217-30.
[41] N.Y. Ignat'eva, N.A. Danilov, S.V. Averkiev, M.V. Obrezkova, V.V. Lunin, E.N. Sobol', Determination of hydroxyproline in tissues and the evaluation of the collagen content of the tissues, J Anal Chem+ 62(1) (2017) 51-57.
[42] P.M. Crapo, T.W. Gilbert, S.F. Badylak, An overview of tissue and whole organ decellularization processes, Biomaterials 32(12) (2011) 3233-43.
[43] J.C. Iatridis, L.A. Setton, M. Weidenbaum, V.C. Mow, The viscoelastic behavior of the non-degenerate human lumbar nucleus pulposus in shear, J Biomech 30(10) (1997) 1005-13.
[44] M. Recuerda, S.P. Cote, I. Villemure, D. Perie, Influence of experimental protocols on the mechanical properties of the intervertebral disc in unconfined compression, J Biomech Eng 133(7) (2011) 071006.
[45] M. Recuerda, D. Perie, G. Gilbert, G. Beaudoin, Assessment of mechanical properties of isolated bovine intervertebral discs from multi-parametric magnetic resonance imaging, BMC Musculoskelet Disord 13 (2012) 195.
[46] J.M. Cloyd, N.R. Malhotra, L. Weng, W. Chen, R.L. Mauck, D.M. Elliott, Material properties in unconfined compression of human nucleus pulposus, injectable hyaluronic acid-based hydrogels and tissue engineering scaffolds, Eur Spine J 16(11) (2007) 1892-8.
[47] S. Umehara, S. Tadano, K. Abumi, K. Katagiri, K. Kaneda, T. Ukai, Effects of degeneration on the elastic modulus distribution in the lumbar intervertebral disc, Spine (Phila Pa 1976) 21(7) (1996) 811-9; discussion 820.
[48] D.H. Cortes, N.T. Jacobs, J.F. DeLucca, D.M. Elliott, Elastic, permeability and swelling properties of human intervertebral disc tissues: A benchmark for tissue engineering, J Biomech 47(9) (2014) 2088-94.
[49] P.A. Levett, F.P. Melchels, K. Schrobback, D.W. Hutmacher, J. Malda, T.J. Klein, A biomimetic extracellular matrix for cartilage tissue engineering centered on photocurable gelatin, hyaluronic acid and chondroitin sulfate, Acta Biomater 10(1) (2014) 214-23.
[50] E.C. Beck, M. Barragan, M.H. Tadros, E.A. Kiyotake, F.M. Acosta, S.L. Kieweg, M.S. Detamore, Chondroinductive Hydrogel Pastes Composed of Naturally Derived Devitalized Cartilage, Ann Biomed Eng 44(6) (2016) 1863-80.
[51] A. Gilpin, Y. Yang, Decellularization Strategies for Regenerative Medicine: From Processing Techniques to Applications, Biomed Res Int (2017).
[52] A.J. Sutherland, E.C. Beck, S.C. Dennis, G.L. Converse, R.A. Hopkins, C.J. Berkland, M.S. Detamore, Decellularized Cartilage May Be a Chondroinductive Material for Osteochondral Tissue Engineering, Plos One 10(5) (2015).
[53] J.P. Guyette, J.M. Charest, R.W. Mills, B.J. Jank, P.T. Moser, S.E. Gilpin, J.R. Gershlak, T. Okamoto, G. Gonzalez, D.J. Milan, G.R. Gaudette, H.C. Ott, Bioengineering Human Myocardium on Native Extracellular Matrix, Circ Res 118(1) (2016) 56-72.
[54] J.J. Mercuri, S.S. Gill, D.T. Simionescu, Novel tissue-derived biomimetic scaffold for regenerating the human nucleus pulposus, J Biomed Mater Res A 96(2) (2011) 422-35.
[55] H. Cao, S.Y. Xu, EDC/NHS-crosslinked type II collagen-chondroitin sulfate scaffold: characterization and in vitro evaluation, J Mater Sci Mater Med 19(2) (2008) 567-75.
[56] J.Y. Lai, Corneal stromal cell growth on gelatin/chondroitin sulfate scaffolds modified at different NHS/EDC molar ratios, Int J Mol Sci 14(1) (2013) 2036-55.
[57] H.J. Meisel, V. Siodla, T. Ganey, Y. Minkus, W.C. Hutton, O.J. Alasevic, Clinical experience in cell-based therapeutics: disc chondrocyte transplantation A treatment for degenerated or damaged intervertebral disc, Biomol Eng 24(1) (2007) 5-21.

[58] A. Hiyama, J. Mochida, T. Iwashina, H. Omi, T. Watanabe, K. Serigano, F. Tamura, D. Sakai, Transplantation of mesenchymal stem cells in a canine disc degeneration model, J Orthop Res 26(5) (2008) 589-600.
[59] G.W. Omlor, H. Bertram, K. Kleinschmidt, J. Fischer, K. Brohm, T. Guehring, M. Anton, W. Richter, Methods to monitor distribution and metabolic activity of mesenchymal stem cells following in vivo injection into nucleotomized porcine intervertebral discs, Eur Spine J 19(4) (2010) 601-12.
[60] F. Mwale, P. Roughley, J. Antoniou, Distinction between the extracellular matrix of the nucleus pulposus and hyaline cartilage: a requisite for tissue engineering of intervertebral disc, Eur Cell Mater 8 (2004) 58-63; discussion 63-4.
[61] E.A. Aisenbrey, S.J. Bryant, The role of chondroitin sulfate in regulating hypertrophy during MSC chondrogenesis in a cartilage mimetic hydrogel under dynamic loading, Biomaterials 190-191 (2019) 51-62.
[62] T. Wang, F. Yang, A comparative study of chondroitin sulfate and heparan sulfate for directing three-dimensional chondrogenesis of mesenchymal stem cells, Stem Cell Res Ther 8(1) (2017) 284.
[63] C.J. Little, W.M. Kulyk, X. Chen, The Effect of Chondroitin Sulphate and Hyaluronic Acid on Chondrocytes Cultured within a Fibrin-Alginate Hydrogel, J Funct Biomater 5(3) (2014) 197-210.
[64] M. Akmal, A. Singh, A. Anand, A. Kesani, N. Aslam, A. Goodship, G. Bentley, The effects of hyaluronic acid on articular chondrocytes, J Bone Joint Surg Br 87(8) (2005) 1143-9.
[65] S. Nishimoto, M. Takagi, S. Wakitani, T. Nihira, T. Yoshida, Effect of chondroitin sulfate and hyaluronic acid on gene expression in a three-dimensional culture of chondrocytes, J Biosci Bioeng 100(1) (2005) 123-6.
[66] G.C. Ingavle, N.H. Dormer, S.H. Gehrke, M.S. Detamore, Using chondroitin sulfate to improve the viability and biosynthesis of chondrocytes encapsulated in interpenetrating network (IPN) hydrogels of agarose and poly(ethylene glycol) diacrylate, J Mater Sci Mater Med 23(1) (2012) 157-70.
[67] J.L.C. van Susante, J. Pieper, P. Buma, T.H. van Kuppevelt, H. van Beuningen, P.M. van Der Kraan, J.H. Veerkamp, W.B. van den Berg, R.P.H. Veth, Linkage of chondroitin-sulfate to type I collagen scaffolds stimulates the bioactivity of seeded chondrocytes in vitro, Biomaterials 22(17) (2001) 2359-69.
[68] M.M. Caron, P.J. Emans, M.M. Coolsen, L. Voss, D.A. Surtel, A. Cremers, L.W. van Rhijn, T.J. Welting, Redifferentiation of dedifferentiated human articular chondrocytes: comparison of 2D and 3D cultures, Osteoarthritis Cartilage 20(10) (2012) 1170-8.
[69] V. Graceffa, C. Vinatier, J. Guicheux, M. Stoddart, M. Alini, D.I. Zeugolis, Chasing Chimeras - The elusive stable chondrogenic phenotype, Biomaterials 192 (2019) 199-225.
[70] G. Schulze-Tanzil, Activation and dedifferentiation of chondrocytes: implications in cartilage injury and repair, Ann Anat 191(4) (2009) 325-38.
[71] S. Nuernberger, N. Cyran, C. Albrecht, H. Redl, V. Vecsei, S. Marlovits, The influence of scaffold architecture on chondrocyte distribution and behavior in matrix-associated chondrocyte transplantation grafts, Biomaterials 32(4) (2011) 1032-40.
[72] A.C. Hall, The Role of Chondrocyte Morphology and Volume in Controlling Phenotype-Implications for Osteoarthritis, Cartilage Repair, and Cartilage Engineering, Curr Rheumatol Rep 21(8) (2019) 38.
[73] J. Parreno, M. Nabavi Niaki, K. Andrejevic, A. Jiang, P.H. Wu, R.A. Kandel, Interplay between cytoskeletal polymerization and the chondrogenic phenotype in chondrocytes passaged in monolayer culture, J Anat 230(2) (2017) 234-248.
[74] D. Huang, Effect of extracellular chondroitin sulfate on cultured chondrocytes, J Cell Biol 62(3) (1974) 881-6.
[75] D. Hachim, T.E. Whittaker, H. Kim, M.M. Stevens, Glycosaminoglycan-based biomaterials for growth factor and cytokine delivery: Making the right choices, J Control Release 313 (2019) 131-147.
[76] R.G. Smock, R. Meijers, Roles of glycosaminoglycans as regulators of ligand/receptor complexes, Open Biol 8(10) (2018).
[77] P.D. Benya, J.D. Shaffer, Dedifferentiated chondrocytes reexpress the differentiated collagen phenotype when cultured in agarose gels, Cell 30(1) (1982) 215-24.

[78] M. Schnabel, S. Marlovits, G. Eckhoff, I. Fichtel, L. Gotzen, V. Vecsei, J. Schlegel, Dedifferentiation-associated changes in morphology and gene expression in primary human articular chondrocytes in cell culture, Osteoarthritis Cartilage 10(1) (2002) 62-70.
[79] T. Hamada, T. Sakai, H. Hiraiwa, M. Nakashima, Y. Ono, H. Mitsuyama, N. Ishiguro, Surface markers and gene expression to characterize the differentiation of monolayer expanded human articular chondrocytes, Nagoya J Med Sci 75(1-2) (2013) 101-11.
[80] D.A. Lowther, M. Natarajan, The influence of glycoprotein on collagen fibril formation in the presence of chondroitin sulphate proteoglycan, Biochem J 127(3) (1972) 607-8.
[81] K. Stuart, A. Panitch, Influence of chondroitin sulfate on collagen gel structure and mechanical properties at physiologically relevant levels, Biopolymers 89(10) (2008) 841-51.